THE JOURNAL OF BIOLOGICAL CHEMISTRY VOL. 286, NO. 37, pp. 32036–32044, September 16, 2011

Toward the Discovery of Effective Polycyclic Inhibitors of α-Synuclein Amyloid Assembly*[S]

Received for publication, March 23, 2011, and in revised form, July 7, 2011 Published, JBC Papers in Press, July 27, 2011, DOI 10.1074/jbc.M111.242958

Gonzalo R. Lamberto[‡1], Valentina Torres-Monserrat[‡], Carlos W. Bertoncini[§2], Xavier Salvatella[§3], Markus Zweckstetter[¶‖4], Christian Griesinger[¶], and Claudio O. Fernández[‡¶5]

From the [‡]Instituto de Biología Molecular y Celular de Rosario, Consejo Nacional de Investigaciones Científicas y Técnicas, Universidad Nacional de Rosario, Suipacha 531, S2002LRK Rosario, Argentina, the [§]Institute for Research in Biomedicine, Baldiri Reixac 10, 08029 Barcelona, Spain, the [¶]Department of NMR-based Structural Biology, Max Planck Institute for Biophysical Chemistry, Am Fassberg 11, D-37077 Göttingen, Germany, and the [‖]Deutsche Forschungsgemeinschaft Center for the Molecular Physiology of the Brain, D-37077 Göttingen, Germany

The fibrillation of amyloidogenic proteins is a critical step in the etiology of neurodegenerative disorders such as Alzheimer and Parkinson diseases. There is major interest in the therapeutic intervention on such aberrant aggregation phenomena, and the utilization of polyaromatic scaffolds has lately received considerable attention. In this regard, the molecular and structural basis of the anti-amyloidogenicity of polyaromatic compounds, required to evolve this molecular scaffold toward therapeutic drugs, is not known in detail. We present here biophysical and biochemical studies that have enabled us to characterize the interaction of metal-substituted, tetrasulfonated phthalocyanines (PcTS) with α-synuclein (AS), the major protein component of amyloid-like deposits in Parkinson disease. The inhibitory activity of the assayed compounds on AS amyloid fibril formation decreases in the order PcTS[Ni(II)] ∼ PcTS > PcTS[Zn(II)] ≫ PcTS[Al(III)] ≈ 0. Using NMR and electronic absorption spectroscopies we demonstrated conclusively that the differences in binding capacity and anti-amyloid activity of phthalocyanines on AS are attributed to their relative ability to self-stack through π-π interactions, modulated by the nature of the metal ion bound at the molecule. Low order stacked aggregates of phthalocyanines were identified as the active amyloid inhibitory species, whose effects are mediated by residue specific interactions. Such sequence-specific anti-amyloid behavior of self-stacked phthalocyanines contrasts strongly with promiscuous amyloid inhibitors with self-association capabilities that act via nonspecific sequestration of AS molecules. The new findings reported here constitute an important contribution for future drug discovery efforts targeting amyloid formation.

The misfolding of proteins into a toxic conformation and their deposition as amyloid-like fibrils are proposed to be at the molecular foundation of a number of neurodegenerative disorders including Creutzfeldt-Jakob, Alzheimer, and Parkinson diseases (1–3). A detailed understanding of the mechanism by which proteins of wide structural diversity are transformed into morphologically similar aggregates is therefore of high clinical importance.

α-Synuclein (AS)[6] is a highly soluble, intrinsically disordered protein, expressed predominantly in the neurons of the central nervous system and localized at presynaptic terminals in close proximity to synaptic vesicles. Evidence that AS amyloidogenesis plays a causative role in the development of Parkinson diseases is furnished by a variety of genetic, neuropathological, and biochemical studies (4–7). Structurally, AS comprises 140 amino acids distributed in three different regions: the amphipathic N terminus (residues 1–60), showing imperfect KTKEGV repeats and involved in lipid binding (8, 9); the highly hydrophobic self-aggregating sequence known as non-Aβ component (residues 61–95), presumed to initiate fibrillation (10); and the acidic C-terminal region (residues 96–140), rich in Pro, Asp, and Glu residues and critical for blocking rapid AS filament assembly (11, 12). In its native monomeric state AS is best described as an ensemble of structurally heterogeneous conformations, with no persistent secondary structure and with long range interresidue interactions that have been shown to stabilize aggregation-autoinhibited conformations (13–15). However, the mechanism(s) underlying the structural transition from the innocuous, monomeric AS to its neurotoxic form still remain poorly described.

The use of aggregation inhibitors as molecular probes of the structural and toxic mechanisms related to amyloid formation

* This work was supported by the Agencia Nacional de Promoción Científica y Tecnológica, Argentina, Fundacíon Antorchas, Max Planck Society, Alexander von Humboldt Foundation, Fundación Josefina Prats, and the Government of Santa Fe. The Bruker Avance II 600 MHz NMR spectrometer used in this work was purchased with funds from ANPCyT (PME2003–2006) and Consejo Nacional de Investigaciones Científicas y Tecnicas, Argentina (CONICET).

[S] The on-line version of this article (available at http://www.jbc.org) contains supplemental Figs. S1–S4.

[1] Recipient of a fellowship from CONICET in Argentina and Fundación Josefina Prats.

[2] Recipient of a Framework Programme 7 Marie Curie Intra-European Fellowship grant.

[3] Supported by Institució Catalana de Recerca i Estudis Avançats, Institute for Research in Biomedicine, Barcelona, Spain, and Ministerio de Ciencia e Innovación de España Grant CTQ2009-08850-BQU.

[4] Supported by the Max Planck Society, Federal Ministry of Education and Research, Germany, Grant NGFN-Plus 01GS08190, and Deutsche Forschungsgemeinschaft Heisenberg Scholarships ZW 71/2-2 and 3-2.

[5] Independent Researcher (CONICET). Head of a Partner Group of the Max Planck Institute for Biophysical Chemistry (Göttingen). To whom correspondence should be addressed. Tel.: 54-341-4448745; Fax: 54-341-4390465; E-mail: cfernan@gwdg.de or fernandez@ibr.gov.ar.

[6] The abbreviations used are: AS, α-synuclein; DMSO, dimethyl sulfoxide; HSQC, heteronuclear single quantum correlation; PcTS, phthalocyanine tetrasulfonate.

has recently become an active area of research (16–29). The identification of aggregation inhibitors and the investigation of their binding modes can therefore constitute an important step toward addressing fundamental issues of amyloid formation and its pathological consequences. Notably, polyaromatic compounds are represented predominantly among hits arising from screenings for anti-amyloidogenic scaffolds (30, 31). One of the most studied polyaromatic aggregation inhibitors is the cyclic tetrapyrrole phthalocyanine tetrasulfonate (PcTS). This compound has been shown to exhibit anti-scrapie activity *in vitro* and *in vivo* (17, 22), disassembling of tau filaments (24), and inhibition of AS filament assembly, leading to the formation of nontoxic AS aggregates (29). We recently elucidated key aspects related to the structural and molecular basis behind the inhibitory interaction of this compound with AS (28). Our study suggested that the core aromatic ring system of the phthalocyanine moiety and the peripheral negatively charged tetrasulfonate groups play a key modulatory role in the anti-amyloidogenic activity that PcTS exerts on AS.

It is well documented that the occupancy of the central core of the tetrapyrrolic ring system in phthalocyanines by different metal cations strongly influences the biological activity of this type of compounds (17, 22, 32–35). Indeed, many metal-substituted phthalocyanines have already been successfully administered to humans in photodynamic and radiotherapy-based cancer treatment protocols, demonstrating a inherent low toxicity (33–35). The key role played by the heterocyclic system of PcTS on inhibition of AS amyloid fibril formation raises then the very important question of how metal ion occupancy may affect the anti-amyloidogenic activity of these molecules. The different properties of the metal ions coordinated into the core aromatic ring of PcTS, such as the residual positive charge located at the metal ion, the preferred coordination stereochemistry of the metal ion, or its relative affinity for axial ligands, might potentially act as critical structural determinants for the interactions of these compounds with target protein sites. Another property of cyclic tetrapyrroles that is modulated by the nature of the coordinated metal ions is their intrinsic propensity to self-associate via aromatic-aromatic stacking interactions (32, 36, 37). This is particularly interesting in the design of anti-amyloid agents because it was recently suggested that self-association could be a common property among aggregation inhibitors found in high throughput screenings (38, 39). However, the hypothesis of a nonspecific anti-amyloid mechanism based on the sequestration of protein molecules by inhibitors with self-association capability contrasts strongly with the direct, specific binding observed for PcTS to AS, and that is expected for biologically active therapeutic candidates. The investigation of the impact of metal ion occupancy on the binding and amyloid inhibitory capacity of phthalocyanines is then crucial to understand fully the structural and mechanistic basis behind its anti-amyloid effect.

In the present study we apply a vast array of biophysical methodologies to investigate the anti-amyloidogenic activity of the metal-loaded phthalocyanines PcTS[Ni(II)], PcTS[Zn(II)], and PcTS[Al(III)] on AS amyloid fibril formation. We report here biochemical and high resolution structural information that demonstrates that the nature of the metal ion coordinated to the central core of the tetrapyrrolic ring determines the mode of interaction and is a key modulator of the anti-amyloidogenic activity of phthalocyanines on AS. We provide conclusive evidence that the binding capacity of phthalocyanines to AS and their anti-amyloid effects exerted on the protein *in vitro* correlate with the propensity of the PcTS species to self-associate. Moreover, our results prove that low order aggregates of PcTS are the active amyloid inhibitory species. The elucidation of molecular and structural determinants on both the protein-inhibitor complex target and the anti-amyloid compound provides relevant information for future drug discovery efforts targeting amyloid formation.

EXPERIMENTAL PROCEDURES

Proteins and Reagents—Unlabeled and ^{15}N-labeled AS species were prepared as described previously (11, 40). The F4A, Y39A, and H50A AS mutants were constructed using the QuikChange site-directed mutagenesis kit (Stratagene) on the AS sequence containing plasmid. The introduced modifications were further verified by DNA sequencing. Purified proteins were dialyzed against working buffer A (20 mM MES, 100 mM NaCl, pH 6.5) supplemented with Chelex (Sigma). PcTS was purchased from MP Biomedicals (Solon, OH); Al(III) phthalocyanine chloride tetrasulfonic acid (PcTS[Al(III)]), Ni(II) phthalocyanine tetrasulfonic acid (PcTS[Ni(II)]), and Zn(II) phthalocyanine tetrasulfonic acid (PcTS[Zn(II)]) were from Frontier Scientific (Logan, UT). $^{15}NH_4Cl$, deuterated MES buffer, and deuterium oxide (D_2O) were purchased from Cambridge Isotope Laboratories (Andover, MA). $ZnSO_4$ salt of the highest purity available was obtained from Sigma.

Aggregation Assays—Aggregation measurements were performed with 100 μM protein samples dissolved in buffer A. Samples were incubated at 37 °C under constant stirring in the absence and presence of 100–300 μM phthalocyanines. The formation of fibrils was estimated from aliquots (5 μl) taken at different time points by use of the standard Thioflavin-T fluorescence assay (41). For the seeding experiments in supplemental Fig. S1, sonicated AS aggregates generated in the absence or presence of different phthalocyanines (4% (v/v)) were added to the aggregation reactions. For the sedimentation analysis shown in Fig. 1*B*, aliquots withdrawn from the aggregation assay were centrifuged at 16,000 × *g* for 10 min. Supernatant fractions, indicative of soluble protein, were resolved by SDS-PAGE and stained with Coomassie Blue. For the detergent-sensitivity studies, aliquots withdrawn from the aggregation assay were centrifuged at 16,000 × *g* for 10 min (Fig. 1*C*). Pellet fractions were incubated for 30 min in 1% Sarkosyl, and the solubilized material was resolved by SDS-PAGE and stained with Coomasie Blue.

NMR Spectroscopy—NMR spectra were acquired on a Bruker Avance II 600 MHz spectrometer using a triple-resonance probe equipped with *z* axis self-shielded gradient coils. Two-dimensional ^{1}H-^{15}N heteronuclear single quantum correlation (HSQC) experiments were performed with pulse field gradient-enhanced pulse sequences on 100 μM ^{15}N-labeled protein samples in buffer A, at 15 °C. ^{1}H-^{15}N HSQC correlation spectra on 10 μM AS samples in the absence or presence of 5 μM phthalocyanines were recorded using the SOFAST-HMQC pulse

sequence. One-dimensional ^{1}H NMR experiments were acquired at 15 °C on 100 μM unlabeled AS dissolved in deuterated buffer A. Aggregation did not occur under these low temperature conditions and absence of stirring. For the mapping experiments, ^{1}H-^{15}N HSQC amide cross-peaks affected during titrations with phthalocyanines were identified by comparing their intensities (I) with those of the same cross-peaks in the dataset of free protein (I_0). The I/I_0 ratios of 95–105 nonoverlapping cross-peaks were plotted as a function of the protein sequence to obtain the intensity profiles. Mean weighted chemical shifts displacements ($MW^{1}H$-$^{15}N\Delta CS$) were calculated as $((\Delta\delta^{1}H)^2 + (\Delta\delta^{15}N)^2/25)^{1/2}$. Pulse field gradient-NMR experiments were acquired at 15 °C on 100 μM unlabeled AS samples dissolved in D_2O and containing dioxane as an internal radius standard (2.12 Å) and viscosity probe. A series of 20 one-dimensional spectra were collected as a function of gradient amplitude. The gradient strength was shifted from 1.69 to 33.72 G cm^{-1} in a linear manner. Acquisition, processing, and visualization of the spectra were performed by using TOPSPIN 2.0 (Bruker), NMRPipe (42), and Sparky.

Electronic Absorption Spectroscopy—Visible electronic absorption spectra of phthalocyanines were recorded at 15 °C using a JASCO V-550 spectrophotometer. Phthalocyanine stock solutions (500 μM) were prepared in DMSO, and measurements were recorded on 5 μM final concentration samples.

Electron Microscopy—Ten-microliter aliquots withdrawn from aggregation reactions were adsorbed onto Formvar/carbon-coated copper grids (Agar Scientific) and negative stained with 2% (w/v) uranyl acetate. Images were obtained at various magnifications (1,000–90,000×) using a Philips CEM100 transmission electron microscope.

RESULTS

Metal-complexed Phthalocyanines Display Different Anti-amyloidogenic Activity—The relative ability of Ni(II)-, Zn(II)-, and Al(III)-bound forms of PcTS to inhibit AS amyloid formation were compared by using SDS-PAGE and transmission electron microscopy (Fig. 1, *A* and *B*). We found that PcTS-[Ni(II)] and PcTS[Zn(II)] produced a variety of smaller, apparently amorphous, nonfibrillar AS species, as well as short, flat fibrillar AS aggregates. Conversely, the AS aggregates in the PcTS[Al(III)]-treated samples showed an amyloid morphology comparable with that of untreated protein samples (Fig. 1*A*). Interestingly, addition of PcTS[Ni(II)], PcTS[Zn(II)], and PcTS[Al(III)] did not significantly reduce the amount of insolubilized AS compared with the nontreated sample (Fig. 1*B*).

Biochemical studies on PcTS[Ni(II)]- and PcTS[Zn(II)]-induced aggregates show that, contrary to amyloid fibrils of AS arising from the nontreated or PcTS[Al(III)] samples, these are more sensitive to dissolution by the mild detergent Sarkosyl (Fig. 1*C*, 48 h). As shown in Fig. 1*C*, 8 h, the treatment with these compounds caused an increased amount of prefibrillar species obtained at the early stages of the assembly process compared with the untreated or PcTS[Al(III)]-treated AS samples. The analysis revealed also that the effect was more pronounced and comparable with that observed for free-PcTS (28), in the presence of PcTS[Ni(II)] (Fig. 1*C*). No evidence of SDS-insoluble AS oligomers, typical of stable off-pathway intermediates, was found in assembly reactions containing Ni(II)- and Zn(II)-loaded phthalocyanines, suggesting that the found prefibrillar structures are likely on-pathway species progressing to amyloid formation. Indeed, the on-pathway nature of PcTS-[Ni(II)]- and PcTS[Zn(II)]-induced AS aggregates was confirmed by their ability to seed amyloid formation of AS (supplemental Fig. S1). No major changes were observed in the rate of aggregation growth, indicating that the nucleation rather than the elongation of amyloid fibrils is the step targeted by the tetrapyrrolic compounds. As expected, AS fibrillar deposits generated in the absence of compounds or in the presence of PcTS[Al(III)] showed a much higher seeding efficiency. Altogether, these results indicate that: (i) differences in the nature of the central metal cation are determinant for the anti-amyloid activity of these tetrapyrrolic compounds; (ii) the anti-amyloid activity of these compounds decreases in the order PcTS[Ni(II)] > PcTS[Zn(II)] ≫ PcTS[Al(III)] ≈ 0; (iii) the mechanism by which PcTS[Ni(II)] and PcTS[Zn(II)] exerts their inhibitory effects parallels that of the metal-free compound (28), which is

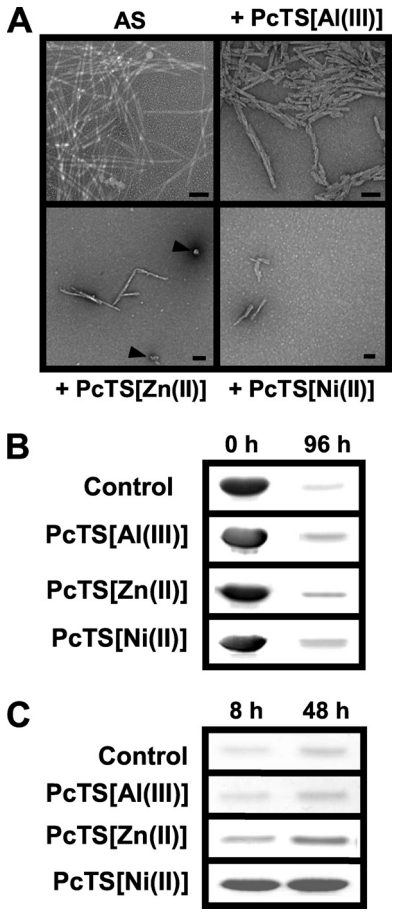

FIGURE 1. **Inhibition of AS amyloid fibril formation by phthalocyanines.** *A*, representative negative stain EM images of AS aggregates (100 μM AS samples) generated in the absence and presence of 300 μM PcTS[Ni(II)], PcTS[Al(III)], and PcTS[Zn(II)] (*scale bars*, 100 nm). Nonfibrillar AS aggregates are indicated by *arrowheads*. *B*, SDS-PAGE of protein remaining soluble at the starting and end points of the aggregation assays in the absence (control) and presence of 300 μM PcTS[Al(III)], PcTS[Zn(II)], or PcTS[Ni(II)]. *C*, Sarkosyl solubilization of pellets during the course of AS aggregation assay, in the absence (control) and presence of 1.0 equivalent of PcTS[Al(III)], PcTS[Zn(II)], and PcTS[Ni(II)].

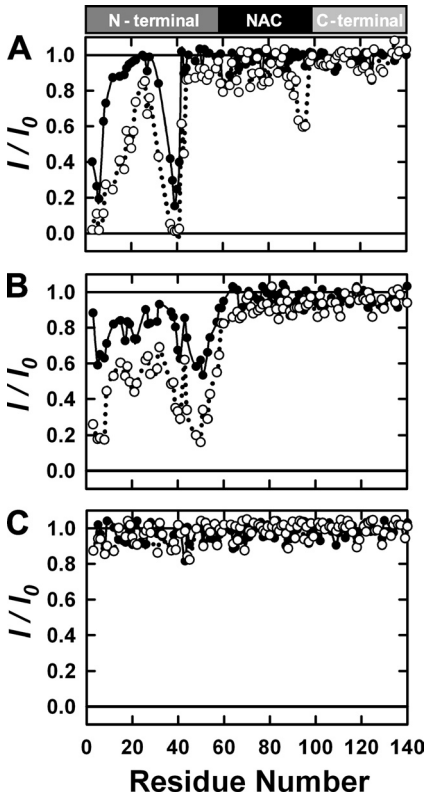

FIGURE 2. **Analysis of phthalocyanines binding to AS by NMR.** I/I_0 profiles of the backbone amide groups of 100 μM AS in the presence of 25 μM (*black*), and 100 μM (*white*) of PcTS[Ni(II)] (*A*), PcTS[Zn(II)] (*B*), and PcTS[Al(III)] (*C*). Broadening effects on AS resonances induced by the paramagnetic metal ion Ni(II) coordinated to PcTS molecules are very weak and can be neglected (50). *NAC*, non-Aβ component.

correlated with the trapping of prefibrillar AS species during the early stages of the assembly process.

The Nature of the Conjugated Metal Ion Influences the Interaction of Phthalocyanines with AS—Such differences in the anti-amyloid activity of the studied phthalocyanines derivatives prompted us to explore details of their binding to AS by NMR spectroscopy. To analyze these interactions, we used ^{1}H-^{15}N HSQC spectroscopy. Titration of AS with increasing concentrations of PcTS[Ni(II)] and PcTS[Zn(II)] caused significant broadening and chemical shift changes in a discrete number of residues at the N-terminal region (Fig. 2, *A* and *B*). No broadening or chemical shift perturbations were observed for the amide groups of residues located in the non-Aβ component or at the C terminus, except by the observation of small broadening and shift perturbation centered in the region 93–95 at high PcTS[Ni(II)] concentrations (100 μM). The nature of the perturbations caused by the metalated-PcTS derivatives on the N-terminal region of AS was similar to that of those induced by the interaction with the metal-free PcTS (28), except for some differences observed for the PcTS[Zn(II)]-AS interactions: (i) the lack of peak broadening or chemical shift perturbation in the 93–95 region; (ii) a clear evidence for the existence of an additional binding site centered in the region 48–53; (iii) the observation of a small signal broadening and chemical shift perturbation centered in the stretch of residues comprising amino acids 18–23. Close analysis of the cross-peaks exhibiting severe broadening effects on AS upon titration with the [Ni(II)] and [Zn(II)] phthalocyanines revealed that they correspond to residues located in the proximity of amino acids with aromatic side chains: a Phe in position 4, a Tyr in position 39, and a His residue in position 50, are all in the regions most affected at the N terminus. The possible involvement of the His-50 residue in a complex seems to be a unique feature of the Zn(II)-metalated PcTS variant. With the aim of determining the role that each of these residues play in directing the binding of PcTS[Ni(II)] and PcTS[Zn(II)] to the N terminus of the protein, we studied a series of aromatic knock-out mutants of AS. Removing the aromatic side chain in positions 4 (F4A variant) (data not shown), 39 (Y39A variant), and 50 (H50A variant) abolished completely the binding of PcTS[Zn(II)] to the 3–9, 35–41, and 48–53 regions of AS, respectively (supplemental Fig. S2, *A* and *B*), highlighting the importance of the aromatic side chains of Phe-4, Tyr-39, and His-50 in the interaction. Interestingly, the small broadening effect centered in the 18–23 sequence was also abolished in the complex of PcTS[Zn(II)] with the H50A mutant. By contrast, the structural features of the PcTS[Ni(II)] interaction with AS remained unaffected upon replacement of His-50 by Ala, confirming the role of only Phe-4 and Tyr-39 as anchoring moieties for the binding of this compound to the N-terminal region (supplemental Fig. S2*C*).

To assess further whether binding of PcTS[Zn(II)] to His-50 may be mediated by coordination of the metal ion to the imidazole ring of the His residue we studied the interaction of the free Zn(II) metal ion with AS. Titration of AS with Zn(II) showed clear perturbations in the region encompassing His-50; however, the most significant chemical shift perturbations were observed on cross-peaks belonging to residues located in the C-terminal region of AS (amino acids 118–129) (supplemental Fig. S3). As expected, the binding features of Zn(II) to the region 48–53 were abolished in the mutant H50A species of AS (data not shown) and were retained in the C-terminal truncated species of AS (1–108 AS). Altogether, our data indicate that the effects observed by PcTS[Zn(II)] in the region comprising this residue are mediated by axial coordination of the imidazole ring of the histidine residue to the PcTS-complexed metal ion. Thus, whereas Zn(II) has the propensity to bind preferentially to the C-terminal region of AS, electrostatic repulsions between the peripheral sulfonate groups in the cyclic tetrapyrrole and the highly negatively charged C-terminal region disfavor the location of the PcTS[Zn(II)] ligand at the C-terminal region.

Notably, when the interaction of AS with PcTS[Al(III)] was analyzed by ^{1}H-^{15}N HSQC spectroscopy, no broadening or chemical shift perturbations could be observed (Fig. 2*C*), even at high ligand:AS ratios (10:1). The fact that neither Tyr-39 nor Phe-4 resonances showed any perturbations indicates that Al(III) substitution renders PcTS unable to interact with AS. These results suggest that a feature intrinsic to the nature of this particular derivative impairs the ability of the tetrapyrrolic moiety to interact with AS and inhibit amyloid formation.

Overall, from the NMR experiments showed here we can conclude that the degree of broadening induced by the studied compounds on the backbone amide resonances of their binding sites decreases in the order PcTS[Ni(II)] $>$ PcTS[Zn(II)] $\gg$ PcTS[Al(III)] $\approx$ 0. The fact that point mutations affect only

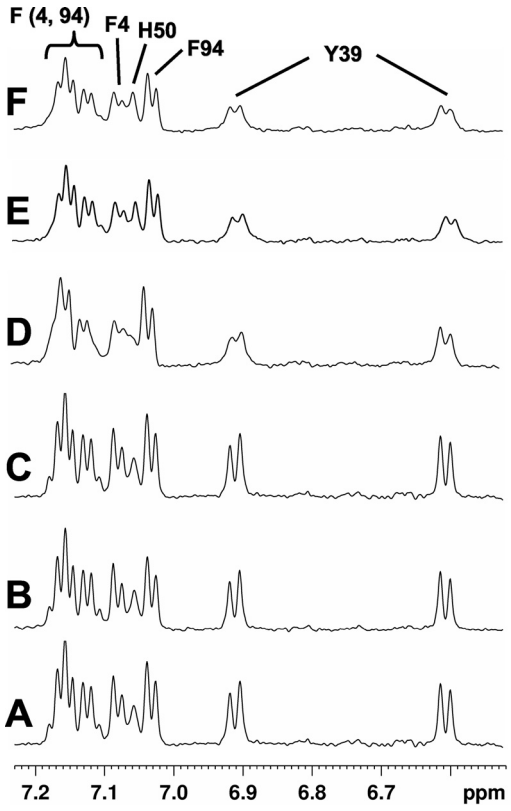

FIGURE 3. **^{1}H NMR of aromatic side chains of 1–108 AS in the presence of phthalocyanines.** Spectra were registered at 15 °C in deuterated buffer A of samples containing 100 μM 1–108 AS (*A*), in the presence of 20 μM PcTS[Al(III)] (*B*), 4 μM PcTS[Zn(II)] (*C*), 20 μM PcTS[Zn(II)] (*D*), 2 μM PcTS[Ni(II)] (*E*), or 2 μM PcTS (*F*). Broadening effects on AS resonances induced by the paramagnetic metal ion Ni(II) coordinated to PcTS molecules are very weak and can be neglected (50).

locally the interaction features of phthalocyanine ligands is a demonstration that the identified binding sites for phthalocyanines constitute independent, noninteractive binding motifs.

Binding Strength and Specificity of Metalated Phthalocyanines to AS—As mentioned above, the ^{1}H-^{15}N HSQC NMR spectrum of AS registered in the presence of metalated phthalocyanines showed a different broadening behavior depending on the nature of the coordinated metal ion. However, the degree of broadening observed on the backbone amide groups of AS in the presence of phthalocyanines might be influenced not only by the interaction of the cyclic tetrapyrroles with aromatic moieties in the protein but also by the occurrence of other structural events such as solvent exchange phenomena triggered by that interaction. Thus, to probe further the different strengths of interaction of phthalocyanine ligands with AS we conducted NMR experiments aimed at detecting directly the selective perturbation of resonances of aromatic side chains upon ligand binding (Fig. 3). The distribution of aromatic residues throughout the AS sequence provides excellent probes for exploring the binding features of cyclic tetrapyrroles to AS. Instead of the full-length protein, we chose to study the 1–108 AS species because the Tyr-rich C-terminal domain does not participate in the binding to PcTS and unnecessarily crowds the spectral region under analysis.

The binding features observed for the PcTS[Ni(II)] and PcTS[Zn(II)] ligands confirm the direct, specific role played by the aromatic side chains of Phe-4, Tyr-39, and His-50 residues of AS in the interaction process (Fig. 3), whereas the broadening behavior is indicative of a system undergoing intermediate chemical or conformational exchange on the NMR time scale (10^{-3} to 10^{-6} s). The titration experiments showed that substantially higher levels of PcTS[Zn(II)] (~10 times higher) are necessary to reproduce the broadening features caused by the metal-free PcTS and the PcTS[Ni(II)] compounds, whereas we did not find perturbations caused by PcTS[Al(III)], confirming the lack of interaction of this ligand with AS at the concentrations assayed (up to 1 mM). This behavior indicates that the strength of interaction of phthalocyanines with AS decrease in the order PcTS[Ni(II)] ~ PcTS > PcTS[Zn(II)] ≫ PcTS-[Al(III)] ≈ 0.

The key role of Tyr-39 in the fibrillation pathway of AS in comparison with the negligible effect that mutations of the His-50 and Phe-4 residues have displayed (supplemental Fig. S4) confirms that specific aromatic interactions with the Tyr-39 residue provide the central mechanistic basis for the inhibitory process of the assayed phthalocyanines (28).

The Interaction of Phthalocyanines with AS Is Mediated by Low Order Stacked Species—To assess the possibility that the distinct tendency of PcTS derivatives to self-associate determines their binding abilities to AS, we compared their tendencies to form stacked aggregates employing electronic absorption spectroscopy. Tetrapyrrolic compounds are known to remain aggregated in aqueous solution while staying monomeric and soluble in organic solvents such as DMSO (32, 43). These features are reflected in their electronic absorption spectral properties as a shift and broadening of the absorptive peaks in the aggregated state compared with the monomeric state (32, 43). PcTS and its derivatives display characteristic absorption bands, named Q bands, centered at approximately 600–700 nm, and the position and extinction coefficient of these bands are therefore a valid reporter of their degree of stacking. Thus, we characterized the aggregation state of metal-free PcTS and the various metalated PcTS derivatives by comparative assessment of the electronic absorption profiles of the compounds in a series of aqueous buffered solutions with increasing DMSO content.

The spectrum of PcTS in buffer A is characterized by a broad band at ~600 nm that is blue-shifted and less intense compared with the spectrum of the monomeric PcTS in DMSO, which exhibits two sharp bands in the range of 650–700 nm (Fig. 4*A*). The spectrum recorded in 50:50% of buffer A:DMSO clearly shows the coexistence of the different species involved in the equilibrium between the pure monomeric and the aggregated state. The electronic absorption spectral properties of PcTS indicate that in aqueous solution the compound is not monomeric, whereas the continuous shift and severe broadening observed for the Q bands in the transition from 100% to 0% DMSO is consistent with a high propensity of the compound to form stacked aggregates in aqueous solution.

The transition from DMSO into buffer A observed for PcTS-[Ni(II)] and PcTS[Zn(II)] (Fig. 4, *B* and *C*) displays spectral features that are similar to those observed for metal-free PcTS; these compounds present in aqueous buffer absorption spectra with a broad absorptive peak, indicative of self-association in

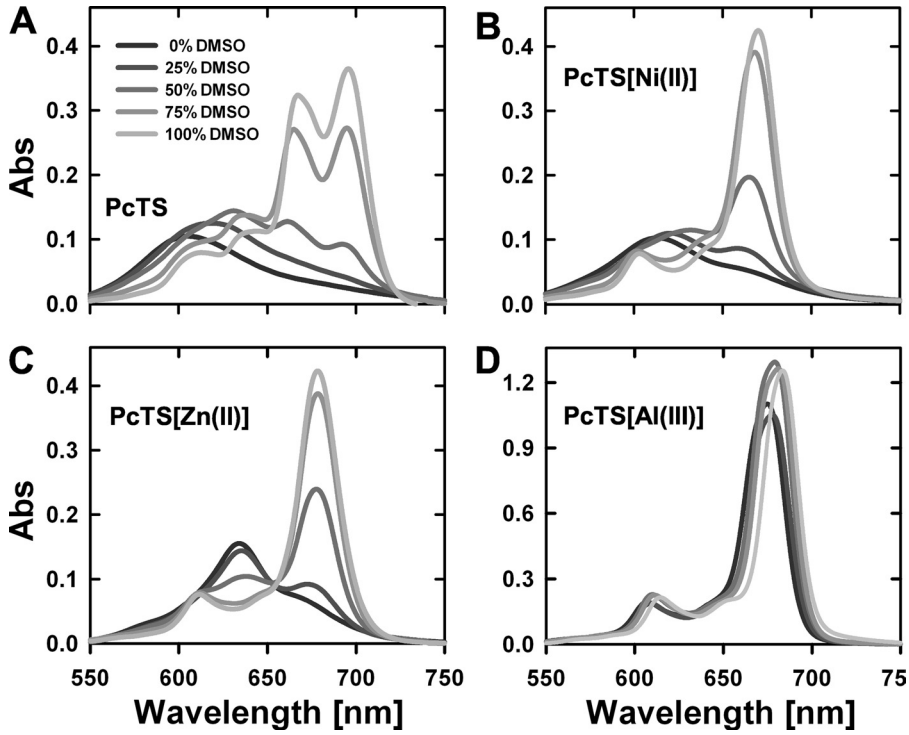

FIGURE 4. **Effect of solvent polarity on electronic absorption spectra of phthalocyanines.** Electronic absorption spectra of PcTS (*A*), PcTS[Ni(II)] (*B*), PcTS[Zn(II)] (*C*), and PcTS[Al(III)] (*D*) are shown. Phthalocyanine solutions (5 μM) were prepared with the designated percentage of DMSO. Buffer A was used as the aqueous solvent.

aqueous media. Similarly to the metal-free PcTS ligand, this peak disappears upon dissolution of the compound in 100% DMSO, giving rise to a single sharp peak in the region 650–700 nm. However, the sharper nature and the less pronounced shift observed for the Q band of the PcTS[Zn(II)] ligand in its transition from 100% to 0% DMSO indicate that this metalated phthalocyanine has less propensity to form stacked aggregates than PcTS[Ni(II)] and its metal-free form. Indeed, a clear isosbestic point attributed to a simple monomer-higher order aggregate equilibrium is observable at ~660 nm in the absorption spectra of PcTS[Zn(II)], indicating that contrary to PcTS-[Ni(II)] or metal-free PcTS, stacked aggregates coexist in equilibrium with a substantial amount of monomeric species in this metal derivative. Interestingly, the spectrum of PcTS[Al(III)] in aqueous buffer exhibits a single major sharp band in the region 650–700 nm and a much less intense band near 610 nm, indicative of a predominant monomeric state of the tetrapyrrolic macrocycle (Fig. 4*D*). Uniquely for PcTS[Al(III)], these spectral characteristics remain essentially constant under all solvent conditions assayed (Fig. 4*D*). Altogether, these data indicate that the relative presence of self-stacked species decreases in the order PcTS[Ni(II)] ~ PcTS > PcTS[Zn(II)] > > PcTS-[Al(III)] ≈ 0.

To assess further the nature of the phthalocyanines species involved in the interaction with AS, we performed NMR experiments at the low micromolar concentrations of phthalocyanines used in the electronic absorption studies. These studies showed that the binding features of Ni(II)- and Zn(II)-loaded phthalocyanines to AS are preserved, confirming that the stacked compound species evidenced by those studies are the main effectors for the interaction with AS (Fig. 5*A*). We then

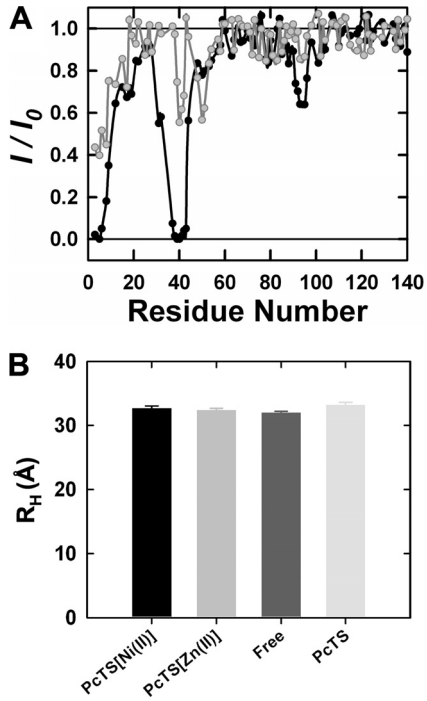

FIGURE 5. **The interaction of phthalocyanines with AS is mediated by low order stacked species.** *A*, I/I_0 profiles of the backbone amide groups of 10 μM AS in the presence of 5 μM PcTS[Zn(II)] (*gray*) or 5 μM PcTS[Ni(II)] (*black*) measured from ^{1}H-^{15}N SOFAST-HMQC correlation experiments. *B*, hydrodynamic radii calculated by pulse field gradient-NMR experiments of 100 μM AS in the absence (*dark gray*) and presence of 1.0 equivalent of PcTS[Ni(II)] (*black*), PcTS[Zn(II)] (*gray*), or PcTS (*light gray*).

employed pulse field gradient-NMR to measure the hydrodynamic properties of AS in the absence and presence of metal-free PcTS and their Ni(II)- and Zn(II)-loaded forms. The effec-

tive R_H of free AS was found to be 32.0 ± 1.0 Å, which is in good agreement with previous reports of the hydrodynamic properties of monomeric AS (44, 45) (Fig. 5*B*). The absence of noticeable changes in the hydrodynamic properties of the protein upon addition of phthalocyanines (Fig. 5*B*) suggests that the formed protein-ligand complexes are of a size similar to that of the free protein. Altogether, these evidences indicate that binding of the studied phthalocyanines to monomeric AS proceeds via interactions with low order stacked species of the compounds.

DISCUSSION

There is considerable interest in developing inhibitors of amyloid formation, both because of their obvious therapeutic potential and because they can provide powerful tools for mechanistic studies (28, 46, 47). Several studies have focused recently on the role of small molecules that interact with AS and inhibit its aggregation-fibrillation *in vitro* and *in vivo* (19, 20, 23, 25–29). Polyphenols, flavonoids, porphyrins, and phthalocyanines are all polyaromatic scaffolds included in this group of compounds. Interestingly, many of these fibrillation inhibitors resemble molecules known to form chemical aggregates like colloidal particles, typically highly conjugated and with a strong hydrophobic character (38, 39). Mechanistically, recent studies proposed that the inhibition of amyloid formation by these compounds might be operated through a protein sequestration-based mechanism rather than by a direct, specific binding that one would ideally expect to find in a suitable therapeutic lead compound (31, 45). To understand fully the way amyloid inhibitors modulate protein aggregation and to distinguish between nonspecific and specific mechanisms, it is of paramount importance to obtain precise atomic level structural information of the molecular complex but also to investigate the intrinsic physicochemical and structural requirements of the inhibitor molecules that are critical for efficient and specific anti-amyloidogenic activity.

In the present work we have demonstrated that metal incorporation into the heterocycle center modulates the anti-amyloidogenic activity of phthalocyanines in various ways. Conjugation with Ni(II) and Zn(II) produces phthalocyanine derivatives that inhibit efficiently the amyloid fibril formation of AS. However, we showed that the PcTS[Al(III)] conjugate does not present an effective action against the fibrillation process of AS. Additionally, the non- or weak paramagnetic nature of the studied phthalocyanines derivatives allowed us to obtain residue specific information of the interaction process by NMR spectroscopy, which otherwise would be precluded by the use of strongly paramagnetic derivatives such as PcTS[Cu(II)] (23). The analysis of NMR data indicates that PcTS[Al(III)] is not able to interact with the protein and that the PcTS[Ni(II)] and PcTS[Zn(II)] ligands, similarly to metal-free PcTS, bind to the aromatic residues Phe-4 and Tyr-39 at the N-terminal region of the protein. A unique feature observed in PcTS[Zn(II)] is the axial coordination of the His-50 imidazole ring through the Zn(II) metal ion. This indicates that the nature of the metal ion conjugated at the center of the porphyrin ring may also influence the binding features of the compound by targeting other sites in the protein. However, the results demonstrated that the structural basis mediating the anti-amyloid effect of PcTS-[Ni(II)] and PcTS[Zn(II)] parallels that of metal-free PcTS, ascribed to the interaction with Tyr-39 (28).

Despite the fact that the nature of the main anchoring groups is shared by PcTS[Ni(II)] and PcTS[Zn(II)], we found indications of significant differences on their relative binding features to these sites. As shown by one- and two-dimensional NMR experiments, much higher concentrations of PcTS[Zn(II)] relative to the Ni(II) form are required to cause a similar line broadening on resonances of the affected aromatic residues, suggesting an extra physicochemical determinant of such behavior. The differences are even more dramatic in the case of the Al(III) derivative, which shows a complete lack of interaction with the protein. To clarify these dissimilarities, we tested the possibility that the distinct self-association tendencies of phthalocyanine derivatives could determine their binding abilities to AS. The self-stacking behavior of the compounds was characterized by electronic absorption spectroscopy in several buffer mixtures of buffer-DMSO and an aqueous buffer alone. Although PcTS[Al(III)] remains as monomer in all assayed media conditions, metal-free PcTS and their Ni(II) and Zn(II)-loaded forms show, in aqueous buffer, the signature spectral properties of self-stacked aggregates. The planarity and aromaticity of the central heterocycle appear to be determining factors for such self-association reactions which, however, can be perturbed or heavily impaired by the nature of the conjugated metal ion (32, 36). Indeed, the compound PcTS[Al(III)], in which the metal ion Al(III) may coordinate axially with an anion (chloride, for instance) gives rise to phthalocyanines with severe distorted structures with an axial out-of-plane atom, preventing the stacking of the PcTS[Al(III)] molecules. The existence of a detectable proportion of monomers in equilibrium with aggregates for the Zn(II) derivative compared with the PcTS and PcTS[Ni(II)] ligands might be then reflecting the differences between slightly distorted and perfect planar phthalocyanines. Altogether, our data show that the relative degree of tetrapyrrole self-stacking is PcTS[Ni(II)] ∼ PcTS > PcTS-[Zn(II)] ≫ PcTS[Al(III)] ≈ 0.

Notably, the degree of phthtalocyanines self-association correlates precisely with their capabilities to bind the Tyr-39 residue of AS and, more importantly, with their activity as amyloid fibrillation inhibitors. Morever, our results prove conclusively that low order aggregates of PcTS are the active amyloid inhibitory species. At this juncture, a comparative analysis with the polyphenolic family of amyloid inhibitors, such as Congo Red and lacmoid, whose inhibitory effects on AS amyloid formation are also mediated by the binding of self-stacked small oligomeric species to the protein (45), can be revealing. In contrast with the well defined binding of active phthalocyanines to specific aromatic residues of AS, the compounds Congo Red and lacmoid were shown to interact with a wide region of the N terminus and central non-Aβ component domain of the monomeric protein. The extensive and general broadening that the compounds caused on the backbone resonances of the first 100 amino acids of AS argue against the occurrence of residue specific ligand-protein interactions (23, 45). Moreover, the broadening beyond detection of resonances belonging to the entire N-terminal amphipathic AS region is reminiscent of the pro-

tein interaction with detergent micelles and lipid vesicles (8). The differences in interaction mechanisms for these compounds are indeed reflected in their anti-amyloid behavior. Although the binding features of Congo Red and lacmoid to AS suggest that the molecular interactions might lead to the conformational stabilization or sequestration of AS monomers and inhibition of the self-assembly process (31, 45), our data reveal that major changes in AS induced by phthalocyanine derivatives are only local and restricted to the immediate vicinity of aromatic residues at the N-terminal region of AS. Thus, the substantial change of aggregation rate and morphology of the resulting species after specific PcTS-mediated perturbation of Tyr-39 would be fully attributable to a loss of function of the aromatic side chain in the AS self-assembly process, rather than due to the nonspecific sequestration of AS molecules or the conformational stabilization of the native state of the protein. Indeed, the core region of amyloid fibrils of AS was shown to begin somewhere in the range of residues 31–39 (48, 49), precisely in the close vicinity of the primary site targeted by phthalocyanines. Specific aromatic interactions between the tetrapyrrolic cycle in the inhibitor molecule and aromatic residues in the amyloidogenic sequence could compromise the earlier intra- and intermolecular interactions necessary for amyloidogenic structural conversions, frustrating formation of the amyloidogenic core and efficiently interfering with fibril assembly. It is noteworthy that interactions governing the protein-compound reactions are of the same nature of those responsible for both compound-compound and protein-protein association reactions.

At this point we can identify two main factors that are able to explain the scarcity of amyloid aggregation inhibitors that have progressed through clinical trials: (i) the lack of precise atomic level structural information of the protein-inhibitor molecular complexes; (ii) the intrinsic complexity of the inhibitory mechanism and the modest research aimed to describe the physicochemical and structural requirements of the inhibitor molecules that are critical for efficient and specific anti-amiloiydogenic activity. Understanding the way amyloid inhibitors modulate protein aggregation and distinguishing between nonspecific and specific mechanisms are then of paramount importance. In this regard, the new findings reported here constitue an important contribution to the development of small molecule inhibitors with enhanced therapeutic effectiveness.

Acknowledgment—C. W. B. thanks Institute for Research in Biomedicine, Barcelona, Spain, for access to equipment.

REFERENCES

1. Chiti, F., and Dobson, C. M. (2006) *Annu. Rev. Biochem.* **75,** 333–366
2. Luheshi, L. M., Crowther, D. C., and Dobson, C. M. (2008) *Curr. Opin. Chem. Biol.* **12,** 25–31
3. Sipe, J. D. (1992) *Annu. Rev. Biochem.* **61,** 947–975
4. Krüger, R., Kuhn, W., Müller, T., Woitalla, D., Graeber, M., Kösel, S., Przuntek, H., Epplen, J. T., Schöls, L., and Riess, O. (1998) *Nat. Genet.* **18,** 106–108
5. Polymeropoulos, M. H., Lavedan, C., Leroy, E., Ide, S. E., Dehejia, A., Dutra, A., Pike, B., Root, H., Rubenstein, J., Boyer, R., Stenroos, E. S., Chandrasekharappa, S., Athanassiadou, A., Papapetropoulos, T., Johnson, W. G., Lazzarini, A. M., Duvoisin, R. C., Di Iorio, G., Golbe, L. I., and Nussbaum, R. L. (1997) *Science* **276,** 2045–2047
6. Spillantini, M. G., Crowther, R. A., Jakes, R., Hasegawa, M., and Goedert, M. (1998) *Proc. Natl. Acad. Sci. U.S.A.* **95,** 6469–6473
7. Spillantini, M. G., Schmidt, M. L., Lee, V. M., Trojanowski, J. Q., Jakes, R., and Goedert, M. (1997) *Nature* **388,** 839–840
8. Bussell, R., Jr., and Eliezer, D. (2003) *J. Mol. Biol.* **329,** 763–778
9. Ulmer, T. S., Bax, A., Cole, N. B., and Nussbaum, R. L. (2005) *J. Biol. Chem.* **280,** 9595–9603
10. Giasson, B. I., Murray, I. V., Trojanowski, J. Q., and Lee, V. M. (2001) *J. Biol. Chem.* **276,** 2380–2386
11. Fernández, C. O., Hoyer, W., Zweckstetter, M., Jares-Erijman, E. A., Subramaniam, V., Griesinger, C., and Jovin, T. M. (2004) *EMBO J.* **23,** 2039–2046
12. Hoyer, W., Cherny, D., Subramaniam, V., and Jovin, T. M. (2004) *Biochemistry* **43,** 16233–16242
13. Bertoncini, C. W., Jung, Y. S., Fernandez, C. O., Hoyer, W., Griesinger, C., Jovin, T. M., and Zweckstetter, M. (2005) *Proc. Natl. Acad. Sci. U.S.A.* **102,** 1430–1435
14. Lee, J. C., Gray, H. B., and Winkler, J. R. (2005) *J. Am. Chem. Soc.* **127,** 16388–16389
15. Lee, J. C., Lai, B. T., Kozak, J. J., Gray, H. B., and Winkler, J. R. (2007) *J. Phys. Chem. B* **111,** 2107–2112
16. Blanchard, B. J., Chen, A., Rozeboom, L. M., Stafford, K. A., Weigele, P., and Ingram, V. M. (2004) *Proc. Natl. Acad. Sci. U.S.A.* **101,** 14326–14332
17. Caughey, W. S., Raymond, L. D., Horiuchi, M., and Caughey, B. (1998) *Proc. Natl. Acad. Sci. U.S.A.* **95,** 12117–12122
18. Chopra, V., Fox, J. H., Lieberman, G., Dorsey, K., Matson, W., Waldmeier, P., Housman, D. E., Kazantsev, A., Young, A. B., and Hersch, S. (2007) *Proc. Natl. Acad. Sci. U.S.A.* **104,** 16685–16689
19. Ehrnhoefer, D. E., Bieschke, J., Boeddrich, A., Herbst, M., Masino, L., Lurz, R., Engemann, S., Pastore, A., and Wanker, E. E. (2008) *Nat. Struct. Mol. Biol.* **15,** 558–566
20. Masuda, M., Suzuki, N., Taniguchi, S., Oikawa, T., Nonaka, T., Iwatsubo, T., Hisanaga, S., Goedert, M., and Hasegawa, M. (2006) *Biochemistry* **45,** 6085–6094
21. Necula, M., Kayed, R., Milton, S., and Glabe, C. G. (2007) *J. Biol. Chem.* **282,** 10311–10324
22. Priola, S. A., Raines, A., and Caughey, W. S. (2000) *Science* **287,** 1503–1506
23. Rao, J. N., Dua, V., and Ulmer, T. S. (2008) *Biochemistry* **47,** 4651–4656
24. Taniguchi, S., Suzuki, N., Masuda, M., Hisanaga, S., Iwatsubo, T., Goedert, M., and Hasegawa, M. (2005) *J. Biol. Chem.* **280,** 7614–7623
25. Zhu, M., Rajamani, S., Kaylor, J., Han, S., Zhou, F., and Fink, A. L. (2004) *J. Biol. Chem.* **279,** 26846–26857
26. Bieschke, J., Russ, J., Friedrich, R. P., Ehrnhoefer, D. E., Wobst, H., Neugebauer, K., and Wanker, E. E. (2010) *Proc. Natl. Acad. Sci. U.S.A.* **107,** 7710–7715
27. Braga, C. A., Follmer, C., Palhano, F. L., Khattar, E., Freitas, M. S., Romão, L., Di Giovanni, S., Lashuel, H. A., Silva, J. L., and Foguel, D. (2011) *J. Mol. Biol.* **405,** 254–273
28. Lamberto, G. R., Binolfi, A., Orcellet, M. L., Bertoncini, C. W., Zweckstetter, M., Griesinger, C., and Fernández, C. O. (2009) *Proc. Natl. Acad. Sci. U.S.A.* **106,** 21057–21062
29. Lee, E. N., Cho, H. J., Lee, C. H., Lee, D., Chung, K. C., and Paik, S. R. (2004) *Biochemistry* **43,** 3704–3715
30. Bulic, B., Pickhardt, M., Schmidt, B., Mandelkow, E. M., Waldmann, H., and Mandelkow, E. (2009) *Angew. Chem. Int. Ed. Engl.* **48,** 1740–1752
31. Feng, B. Y., Toyama, B. H., Wille, H., Colby, D. W., Collins, S. R., May, B. C., Prusiner, S. B., Weissman, J., and Shoichet, B. K. (2008) *Nat. Chem. Biol.* **4,** 197–199
32. Caughey, W. S., Priola, S. A., Kocisko, D. A., Raymond, L. D., Ward, A., and Caughey, B. (2007) *Antimicrob. Agents Chemother.* **51,** 3887–3894
33. Hill, J. S., Kahl, S. B., Stylli, S. S., Nakamura, Y., Koo, M. S., and Kaye, A. H. (1995) *Proc. Natl. Acad. Sci. U.S.A.* **92,** 12126–12130
34. Stylli, S., Hill, J., Sawyer, W., and Kaye, A. (1995) *J. Clin. Neurosci.* **2,** 146–151
35. Stylli, S. S., Hill, J. S., Sawyer, W. H., and Kaye, A. H. (1995) *J. Clin. Neurosci.* **2,** 64–72
36. Boyle, R. W., and Dolphin, D. (1996) *Photochem. Photobiol.* **64,** 469–485

37. Gantchev, T. G., Ouellet, R., and van Lier, J. E. (1999) *Arch. Biochem. Biophys.* **366,** 21–30
38. McGovern, S. L., Caselli, E., Grigorieff, N., and Shoichet, B. K. (2002) *J. Med. Chem.* **45,** 1712–1722
39. McGovern, S. L., Helfand, B. T., Feng, B., and Shoichet, B. K. (2003) *J. Med. Chem.* **46,** 4265–4272
40. Hoyer, W., Cherny, D., Subramaniam, V., and Jovin, T. M. (2004) *J. Mol. Biol.* **340,** 127–139
41. Nilsson, M. R. (2004) *Methods* **34,** 151–160
42. Delaglio, F., Grzesiek, S., Vuister, G. W., Zhu, G., Pfeifer, J., and Bax, A. (1995) *J. Biomol. NMR* **6,** 277–293
43. Laia, C. A., and Costa, S. M. (2008) *J. Phys. Chem. B* **112,** 4276–4282
44. Bertoncini, C. W., Rasia, R. M., Lamberto, G. R., Binolfi, A., Zweckstetter, M., Griesinger, C., and Fernandez, C. O. (2007) *J. Mol. Biol.* **372,** 708–722
45. Lendel, C., Bertoncini, C. W., Cremades, N., Waudby, C. A., Vendruscolo, M., Dobson, C. M., Schenk, D., Christodoulou, J., and Toth, G. (2009) *Biochemistry* **48,** 8322–8334
46. Abedini, A., Meng, F., and Raleigh, D. P. (2007) *J. Am Chem. Soc.* **129,** 11300–11301
47. Yan, L. M., Tatarek-Nossol, M., Velkova, A., Kazantzis, A., and Kapurniotu, A. (2006) *Proc. Natl. Acad. Sci. U.S.A.* **103,** 2046–2051
48. Der-Sarkissian, A., Jao, C. C., Chen, J., and Langen, R. (2003) *J. Biol. Chem.* **278,** 37530–37535
49. Heise, H., Hoyer, W., Becker, S., Andronesi, O. C., Riedel, D., and Baldus, M. (2005) *Proc. Natl. Acad. Sci. U.S.A.* **102,** 15871–15876
50. Bertini, I., and Luchinat, C. (1996) in *NMR of Paramagnetic Substances* (Lever, A. B. P., ed) Coordination Chemistry Review, Aniversary Volume Number 150, pp. 77–110, Elseiver, Amsterdam